Electronic structure and transport for a laser-field-irradiated quantum wire with Rashba spin–orbit coupling

2006 J. Phys.: Condens. Matter 18 9161

(http://iopscience.iop.org/0953-8984/18/40/003)

INSTITUTE OF PHYSICS PUBLISHING JOURNAL OF PHYSICS: CONDENSED MATTER

J. Phys.: Condens. Matter **18** (2006) 9161–9171 doi:10.1088/0953-8984/18/40/003

Electronic structure and transport for a laser-field-irradiated quantum wire with Rashba spin–orbit coupling

Guanghui Zhou[1,2,3,4] **and Wenhu Liao**[2]

[1] CCAST (World Laboratory), PO Box 8730, Beijing 100080, People's Republic of China
[2] Department of Physics, Hunan Normal University, Changsha 410081, People's Republic of China
[3] International Center for Materials Physics, Chinese Academy of Sciences, Shenyang 110015, People's Republic of China

E-mail: ghzhou@hunnu.edu.cn

Received 16 May 2006, in final form 6 September 2006
Published 22 September 2006
Online at stacks.iop.org/JPhysCM/18/9161

Abstract

We investigate theoretically the electronic structure and transport for a two-level quantum wire with Rashba spin–orbit coupling (SOC) under the irradiation of an external laser field at low temperatures. The photon-induced transitions between SOC-split subbands with the same lateral confinement quantum number and between subbands with different confinement quantum numbers are expected. Using the method of equation of motion (EOM) for Keldysh nonequilibrium Green's functions (NGF), we examine the time-averaged density of states (DOS) and the spin-polarized conductance for the system with photon polarization perpendicular to the wire direction. Through the analytical analysis and some numerical examples, the interplay effects of the external laser field and the Rashba SOC on both the DOS and the conductance of the system are demonstrated and discussed. It is found that the external laser field can adjust the spin polarization rate and the transport of the quantum wire system with some appropriate Rashba SOC strengths.

1. Introduction

In recent years, the effects of SOC in semiconductor mesoscopic systems have attracted more and more attention, since it has played an important role in the emerging field of spintronics (see recent review article [1] and references therein) since the proposal of constructing an

[4] Address for correspondence: Department of Physics, Hunan Normal University, Changsha 410081, People's Republic of China.

electronic analogue of an optic modulator using ferromagnetic contacts as the spin injector and the detector [2]. Many fundamental and interesting phenomena, such as spin precession [3, 4], spin accumulation [5, 6], spin (polarized) transport [7, 8] and spin Hall effect [9, 10], in the systems with SOC have been investigated and are under further study now. Though the SOC has its origin in relativistic effects, it is regarded as vital in some low-dimensional mesoscopic semiconductor systems [11, 12].

Usually, two types of SOC are taken into account in the investigation for systems based on a two-dimensional electron gas (2DEG) confined in a semiconductor heterostructure. They are Rashba [11] and Dresselhaus [12] SOC, which can be described by the Hamiltonians

$$H_{\mathrm{R}} = \frac{\hbar k_{\mathrm{R}}}{m^*}(\sigma_x p_y - \sigma_y p_x) \tag{1}$$

and

$$H_{\mathrm{D}} = \frac{\hbar k_{\mathrm{D}}}{m^*}(\sigma_y p_y - \sigma_x p_x), \tag{2}$$

respectively, where m^* is the effective electron mass and $\boldsymbol{\sigma} = (\sigma_x, \sigma_y, \sigma_z)$ is the vector of the Pauli matrix. The strengths of the two types of SOC are measured in terms of characteristic wavevectors k_{R} and k_{D}, respectively. For some semiconductor-based systems (e.g. InAs quantum well), the Rashba term arising from the structure inversion asymmetry in heterostructures [13, 14] is roughly one order magnitude larger than the Dresselhaus term, which is due to the bulk inversion asymmetry [15]. Moreover, the strength of Rashba SOC can be tuned by the external gate voltage [16], and its effect on the systems has been paid more attention, particularly in the quasi-one-dimensional quantum wire system.

Mesoscopic systems with or without external magnetic field in the presence of SOC have been studied extensively [3–10, 17]. Two years ago, two independent experiments on (001)-grown n-type GaAs multiple quantum well structures had been done by using circularly polarized infrared radiation [18] and two orthogonally polarized optical harmonic pulses [19], respectively. The spin photon current [18] and the pure spin current [19] due to resonant intersubband transitions have been observed in the absence of any external magnetic field. Hereafter, for a single quantum well (2DEG) with SOC irradiated under in-plane linearly polarized infrared irradiation, the spin-dependent density of state (DOS) and the density of spin polarization has been calculated, and a pure spin current has been theoretically verified for the system [20]. Further, a mechanism for spin-polarized photocurrent generation in a multimode quantum wire, which is due to the combined effect of the Rashba SOC and a linearly polarized in-plane microwave irradiation, has been proposed in the presence of a static in-plane magnetic field [21]. On the other hand, the electron transport for a quantum wire under time-varying electromagnetic (EM) field irradiation in the absence of SOC has been analysed previously by means of the NGF [22] and the scattering matrix approach [23], respectively. However, further confined low-dimensional systems, such as a two-level quasi-one-dimensional quantum wire or quasi-zero-dimensional quantum dot with SOC under the irradiation of a time-dependent field, have been studied rarely [21].

A mesoscopic two-level system (such as a two-level quantum wire or quantum dot) is physically important since it has been proved to be very useful in describing many aspects of interaction between an EM field and the electrons confined in a heterostructure, and in application of solid-state electronic devices. Therefore, it is meaningful to investigate the interplay effect between the SOC and the applied laser field for a two-level mesoscopic system.

In order to investigate the electronic structure and transport of a two-level quantum wire with SOC under an intense laser field irradiation, in this paper we theoretically calculate the time-averaged DOS and the conductance at low temperatures for the system. The interplay

effects of different laser frequencies and Rashba SOC strengths on the electronic structure and transport are investigated by using the nonequilibrium Keldysh formulism (NKF). Through the analysis with a few numerical examples, we find some characteristics different from those for the similar systems in previous works [20–23].

The remainder of the paper is organized as follows. In section 2, we introduce the model Hamiltonian for our system and give the NKF straightforwardly, where the time-averaged DOS and the conductance are calculated analytically. The numerical results and the discussion are shown in section 3. Finally, section 4 concludes the paper.

2. Model and formalism

The NGF approach has been employed in recent decades to study a variety of problems beyond the linear response regime [22]. Meir *et al* [24] derived a formula for the current through a region of interacting electrons using the NKF. Changing the one-direction time axis into a loop with two branches, four Green's functions depending on the relative positions of t_a and t_b in the loop can be defined. They are time-ordered, anti-time-ordered and two distribution Green's functions, respectively. However, only two of them are independent. We will use the approach of the standard nonequilibrium Keldysh EOM in the present work.

Consider a quasi-one-dimensional system of electrons (a quantum wire) in the presence of SOC and an external time-dependent laser field, the model Hamiltonian reads

$$H = \frac{\mathbf{p}^2}{2m^*} + V(\mathbf{r}) + H_{\rm so} + V(t), \tag{3}$$

where $\mathbf{r} = (x, y)$ and $\mathbf{p} = (p_x, p_y)$ are two-dimensional position and momentum vectors, respectively. The SOC Hamiltonian $H_{\rm so}$ generally consists of $H_{\rm R}$ and $H_{\rm D}$, while $V(t)$ is the potential from the interaction of the external time-dependent laser field with electrons in the system. The electrons are confined in the y direction by an infinite square-well potential of width a, i.e.,

$$V(\mathbf{r}) = \begin{cases} 0 & (|y| < a/2) \\ \infty & (|y| > a/2), \end{cases} \tag{4}$$

which can eliminate the possibility of SOC due to the effective electric field coming from the nonuniformity of the confining potential [25].

To investigate the effects of SOC and the external field on the electron transport properties by means of NKF, we rewrite Hamiltonian (3) in the second-quantized form. For this purpose, we define that $a^\dagger_{ks\alpha}$ ($a_{ks\alpha}$) creates (annihilates) an electron with wavevector k and a spin branch s ($s = \uparrow$ and $\downarrow$, or $+$ and $-$, which is the spin branch index corresponding to spin up and spin down, respectively: see equation (11) for a detailed explanation) in mode α in either the left (L) or the right (R) lead, and $c^\dagger_{k_x ns}$ ($c_{k_x ns}$) creates (annihilates) an electron in the nth transverse mode $|k_x, n, s\rangle$ with wavevector k_x and a spin branch index s in the absence of SOC in the quantum wire modelled as a two-level ($n = 1, 2$) system. For convenience, we choose [25] the spin polarization axis $\hat{\mathbf{n}} = (\cos\varphi, \sin\varphi)$ to be along the effective magnetic field due to the SOC for a wave propagating in the x-direction such that

$$|s\rangle = \frac{1}{\sqrt{2}} \begin{pmatrix} s\mathrm{e}^{-\mathrm{i}\varphi/2} \\ \mathrm{e}^{\mathrm{i}\varphi/2} \end{pmatrix} \tag{5}$$

with $\varphi \equiv \arg[k_{\rm D} + \mathrm{i}k_{\rm R}]$. With these definitive operators and spin states, the Hamiltonian for a laser-field-irradiated two-level quantum wire (connected to two electrode leads) in the presence

of SOC reads

$$H = \sum_{k,s,\alpha\in \mathrm{L/R}} \varepsilon_{ks\alpha} a^{\dagger}_{ks\alpha} a_{ks\alpha} + \sum_{k_x,n,s} \varepsilon_{ns}(k_x) c^{\dagger}_{k_x ns} c_{k_x ns} + \sum_{k,k_x,n,s,\alpha\in \mathrm{L/R}} (T^{\alpha}_{kk_x ns} a^{\dagger}_{ks\alpha} c_{k_x ns} + \mathrm{h.c.}) + \sum_{k_x,n,n',s,s'} [\gamma_{nn'}\beta_{ss'} + V_{nsn's'}\cos(\Omega t)] c^{\dagger}_{k_x ns} c_{k_x n's'}, \tag{6}$$

where $\varepsilon_{ks\alpha}$ is the energy level with spin s and wavevector k in lead α, and

$$\varepsilon_{ns}(k_x) = \frac{\hbar^2}{2m^*}\left[(k_x - sk_{\mathrm{so}})^2 + \left(\frac{n\pi}{a}\right)^2\right] - \Delta_{\mathrm{so}} \tag{7}$$

is the nth sublevel in the wire with $k_{\mathrm{so}} = \sqrt{k_{\mathrm{R}}^2 + k_{\mathrm{D}}^2}$ and $\Delta_{\mathrm{so}} = \hbar^2 k_{\mathrm{so}}^2/2m$. In Hamiltonian (6), the coupling between the electrode leads and the wire with strength $T^{\alpha}_{kk_x ns}$ is represented by the third term, and the last term describes the adiabatic electron–photon interaction in the wire [22, 26] and the mixture of transverse modes due to SOC, where $V_{nsn's'}$ are the dipole electron–photon interaction matrix elements (MEs) and Ω the incident laser frequency. Since the frequencies of interest are in the range corresponding to wavelengths of the order of hundreds of nanometres, the spatial variation of the field potential can be neglected. The SOC mixes the transverse modes through the matrix element $\gamma_{nn'}\beta_{ss'}$, where

$$\gamma_{nn'} = \frac{4nn'}{a(n^2 - n'^2)} \begin{cases} (-1)^{\frac{n+n'-1}{2}} & (n \neq n') \\ 0 & (n = n'), \end{cases} \tag{8}$$

and according to the lateral confinement potential [25] $\beta_{ss'}$ is the element of matrix

$$\beta = \frac{\hbar^2}{m^* k_{\mathrm{so}}} \begin{bmatrix} 2\mathrm{i}k_{\mathrm{R}}k_{\mathrm{D}} & k_{\mathrm{D}}^2 - k_{\mathrm{R}}^2 \\ k_{\mathrm{R}}^2 - k_{\mathrm{D}}^2 & -2\mathrm{i}k_{\mathrm{R}}k_{\mathrm{D}} \end{bmatrix}. \tag{9}$$

In the above Hamiltonian we have neglected electron–electron interactions since their effect on SOC can be plausibly taken into a renormalized SOC constant [27].

For simplicity, we focus on the Rashba SOC effect, i.e. let $k_{\mathrm{D}} = 0$. Furthermore, according to the Dyson equation, the coupling between the electrode leads and the wire only adds a self-energy term in the NGF, so we firstly calculate the Green's function (GF) of the quantum wire without considering the electrode leads. In this case the Hamiltonian of the quantum wire part in the absence of EM field reads

$$H_{\mathrm{wire}} = \sum_{k_x} [\varepsilon_{1\uparrow}(k_x) c^{\dagger}_{k_x 1\uparrow} c_{k_x 1\uparrow} + \varepsilon_{1\downarrow}(k_x) c^{\dagger}_{k_x 1\downarrow} c_{k_x 1\downarrow} + \varepsilon_{2\uparrow}(k_x) c^{\dagger}_{k_x 2\uparrow} c_{k_x 2\uparrow} + \varepsilon_{2\downarrow}(k_x) c^{\dagger}_{k_x 2\downarrow} c_{k_x 2\downarrow} + \varepsilon_{\mathrm{R}}(c^{\dagger}_{k_x 2\uparrow} c_{k_x 1\downarrow} + c^{\dagger}_{k_x 1\downarrow} c_{k_x 2\uparrow} - c^{\dagger}_{k_x 1\uparrow} c_{k_x 2\downarrow} - c^{\dagger}_{k_x 2\downarrow} c_{k_x 1\uparrow})], \tag{10}$$

where $\varepsilon_{\mathrm{R}} = 8\hbar^2 k_{\mathrm{R}}/(3m^* a)$. According to equation (5), here the spin-up state $|\uparrow\rangle$ and the spin-down state $|\downarrow\rangle$ are the linear combination of the eigenstates of σ_z

$$\begin{aligned} |\uparrow\rangle &= \frac{1-\mathrm{i}}{2}\begin{pmatrix} 1 \\ 0 \end{pmatrix} + \frac{1+\mathrm{i}}{2}\begin{pmatrix} 0 \\ 1 \end{pmatrix}, \\ |\downarrow\rangle &= -\frac{1-\mathrm{i}}{2}\begin{pmatrix} 1 \\ 0 \end{pmatrix} + \frac{1+\mathrm{i}}{2}\begin{pmatrix} 0 \\ 1 \end{pmatrix}, \end{aligned} \tag{11}$$

with equal probability occupying the real spin-up and spin-down states in the original spin space, respectively.

For definiteness, we consider the case of the applied incident laser polarized along the y direction (perpendicular to the wire direction), hence the diagonal electron–photon interaction MEs are simply zero in the dipole approximation. Also for simplicity in calculation we assume phenomenologically that the off-diagonal electron–photon interaction MEs $V_{1s2s'} =$

$V_{2s1s'} = 1.0$ as the free input parameters (dependent on incident laser intensity), and thus the Hamiltonian (10) becomes

$$\begin{aligned} H'_{\text{wire}} = \sum_{k_x} \{ & \varepsilon_{1\uparrow}(k_x) c^{\dagger}_{k_x 1\uparrow} c_{k_x 1\uparrow} + \varepsilon_{1\downarrow}(k_x) c^{\dagger}_{k_x 1\downarrow} c_{k_x 1\downarrow} + \varepsilon_{2\uparrow}(k_x) c^{\dagger}_{k_x 2\uparrow} c_{k_x 2\uparrow} + \varepsilon_{2\downarrow}(k_x) c^{\dagger}_{k_x 2\downarrow} c_{k_x 2\downarrow} \\ & + [\tfrac{1}{2}(\mathrm{e}^{\mathrm{i}\Omega t} + \mathrm{e}^{-\mathrm{i}\Omega t}) + \varepsilon_{\mathrm{R}}](c^{\dagger}_{k_x 1\downarrow} c_{k_x 2\uparrow} + c^{\dagger}_{k_x 2\uparrow} c_{k_x 1\downarrow}) \\ & + [\tfrac{1}{2}(\mathrm{e}^{\mathrm{i}\Omega t} + \mathrm{e}^{-\mathrm{i}\Omega t}) - \varepsilon_{\mathrm{R}}](c^{\dagger}_{k_x 1\uparrow} c_{k_x 2\downarrow} + c^{\dagger}_{k_x 2\downarrow} c_{k_x 1\uparrow}) \\ & + \tfrac{1}{2}(\mathrm{e}^{\mathrm{i}\Omega t} + \mathrm{e}^{-\mathrm{i}\Omega t})(c^{\dagger}_{k_x 1\uparrow} c_{k_x 2\uparrow} + c^{\dagger}_{k_x 2\uparrow} c_{k_x 1\uparrow} + c^{\dagger}_{k_x 1\downarrow} c_{k_x 2\downarrow} + c^{\dagger}_{k_x 2\downarrow} c_{k_x 1\downarrow}) \}. \end{aligned} \tag{12}$$

It is seen from equations (10) and (12) that the pure Rashba SOC induces spin-flip transitions with equal probabilities (spin conserving) according to equation (6), while the applied laser field may arouse unequal probability transitions for spin flip and spin conserving due to the interplay between the Rashba SOC and the field. Our interest is to numerically find which kind of transition is favourable for this system.

Next we employ the usually defined retarded GF [22, 24]

$$G^r_{nsn's'}(t_2, t_1) = \langle\langle c_{k_x ns}(t_2), c_{k_x n's'}(t_1) \rangle\rangle^r = -\mathrm{i}\theta(t_2 - t_1)\langle\{c_{k_x ns}(t_2), c_{k_x n's'}(t_1)\}\rangle, \tag{13}$$

then its corresponding Keldysh EOM is

$$\begin{aligned} \mathrm{i}\frac{\partial}{\partial t_2}\langle\langle c_{k_x ns}(t_2), c_{k_x n's'}(t_1) \rangle\rangle^r &= \delta(t_2 - t_1)\langle\{c_{k_x ns}(t_2), c_{k_x n's'}(t_1)\}\rangle \\ &+ \langle\langle [c_{k_x ns}(t_2), H], c_{k_x n's'}(t_1) \rangle\rangle^r. \end{aligned} \tag{14}$$

Inserting system Hamiltonian (12) into (14) and transforming the variables to $t_2 - t_1$ and t_1, and then performing the Fourier transform to change the variable $t_2 - t_1$ into ω, we finally obtain the diagonal MEs of the two retarded GFs without the coupling between the electrode leads and the wire

$$\{[\omega - \varepsilon_{1/2\uparrow}(k_x)][\omega - \varepsilon_{2/1\downarrow}(k_x)] - \varepsilon_{\mathrm{R}}^2\}\langle\langle c_{k_x 1/2\uparrow}, c^{\dagger}_{k_x 1/2\uparrow} \rangle\rangle^r_{\omega} = \omega - \varepsilon_{2/1\downarrow}(k_x), \tag{15}$$

$$\{[\omega - \varepsilon_{1/2\downarrow}(k_x)][\omega - \varepsilon_{2/1\uparrow}(k_x)] - \varepsilon_{\mathrm{R}}^2\}\langle\langle c_{k_x 1/2\downarrow}, c^{\dagger}_{k_x 1/2\downarrow} \rangle\rangle^r_{\omega} = \omega - \varepsilon_{2/1\uparrow}(k_x), \tag{16}$$

$$\begin{aligned} [\omega - \varepsilon_{1/2\uparrow}(k_x)]\langle\langle c_{k_x 1/2\uparrow}, c^{\dagger}_{k_x 1/2\uparrow}(t_1) \rangle\rangle^r_{\omega} &= 1 \mp \varepsilon_{\mathrm{R}}\langle\langle c_{k_x 2/1\downarrow}, c^{\dagger}_{k_x 1/2\uparrow}(t_1) \rangle\rangle^r_{\omega} \\ &+ \tfrac{1}{2}\mathrm{e}^{\mathrm{i}\Omega t_1}[\langle\langle c_{k_x 2/1\downarrow}, c^{\dagger}_{k_x 1/2\uparrow}(t_1) \rangle\rangle^r_{\omega+\Omega} + \langle\langle c_{k_x 2/1\uparrow}, c^{\dagger}_{k_x 1/2\uparrow}(t_1) \rangle\rangle^r_{\omega+\Omega}] \\ &+ \tfrac{1}{2}\mathrm{e}^{-\mathrm{i}\Omega t_1}[\langle\langle c_{k_x 2/1\downarrow}, c^{\dagger}_{k_x 1/2\uparrow}(t_1) \rangle\rangle^r_{\omega-\Omega} + \langle\langle c_{k_x 2/1\uparrow}, c^{\dagger}_{k_x 1/2\uparrow}(t_1) \rangle\rangle^r_{\omega-\Omega}], \end{aligned} \tag{17}$$

$$\begin{aligned} [\omega - \varepsilon_{1/2\downarrow}(k_x)]\langle\langle c_{k_x 1/2\downarrow}, c^{\dagger}_{k_x 1/2\downarrow}(t_1) \rangle\rangle^r_{\omega} &= 1 \pm \varepsilon_{\mathrm{R}}\langle\langle c_{k_x 2/1\uparrow}, c^{\dagger}_{k_x 1/2\downarrow}(t_1) \rangle\rangle^r_{\omega} \\ &+ \tfrac{1}{2}\mathrm{e}^{\mathrm{i}\Omega t_1}[\langle\langle c_{k_x 2/1\uparrow}, c^{\dagger}_{k_x 1/2\downarrow}(t_1) \rangle\rangle^r_{\omega+\Omega} + \langle\langle c_{k_x 2/1\downarrow}, c^{\dagger}_{k_x 1/2\downarrow}(t_1) \rangle\rangle^r_{\omega+\Omega}] \\ &+ \tfrac{1}{2}\mathrm{e}^{-\mathrm{i}\Omega t_1}[\langle\langle c_{k_x 2/1\uparrow}, c^{\dagger}_{k_x 1/2\downarrow}(t_1) \rangle\rangle^r_{\omega-\Omega} + \langle\langle c_{k_x 2/1\downarrow}, c^{\dagger}_{k_x 1/2\downarrow}(t_1) \rangle\rangle^r_{\omega-\Omega}], \end{aligned} \tag{18}$$

for spin up and spin down, respectively. It is seen from equations (17) and (18) that the retard NGF G^r_0 with frequency ω is coupled to the components with photon sideband frequencies of $\omega + \Omega$ and $\omega - \Omega$ in connection with k_{so} (the characteristic wavevector of Rashba SOC).

On the other hand, the self-energy describing the influence of the leads on the system can be simply written as

$$\Sigma_{nn'} \equiv \Sigma^{\mathrm{L/R}}_{nn'}(\omega) = 2\pi \sum_{k,k_x,s} (T^{\alpha}_{kk_x ns})^* T^{\alpha}_{k,k_x n's} \delta(\omega - \varepsilon_{ks\alpha}), \tag{19}$$

with which one can construct the GF $G^r = [(G^r_0)^{-1} - \mathrm{i}\Sigma]^{-1}$ for the whole system. If we calculate the time-averaged NGF up to the second order, then at low temperatures the time-averaged DOS is

$$\mathrm{DOS} = -\frac{1}{\pi}\mathrm{Im}[\mathrm{Tr}(G^r(\omega, \omega))], \tag{20}$$

and the conductance has the Landauer-type form [22, 26]

$$G = \frac{e^2}{h}\mathrm{Tr}[\Sigma^{\mathrm{L}}(\omega)G^a(\omega,\omega)\Sigma^{\mathrm{R}}(\omega)G^r(\omega,\omega)]. \tag{21}$$

Here $G^r(\omega,\omega)$ and $G^a(\omega,\omega)$ represent the time-averaged retarded and advanced GFs, respectively.

3. Numerical results and discussion

In the following, we present some numerical examples of the DOS and conductance calculated according to equations (15)–(21) for the system. In our numerical examples, the physical quantities are chosen to be those in InAs semiconductor heterostructures with Rashba SOC characteristic energy $\Delta_{\mathrm{so}} = 1.9$ meV, and SOC constant $\alpha = 4.5 \times 10^{-11}$ eV m, Rashba characteristic wavevector $k_{\mathrm{R}} = 2m^*\alpha/\hbar^2 = 4.2\times10^7$ m^{-1}, effective mass $m^* = 0.036m_e$ [21]. We have selected the hard-wall transverse confining potential with width $a = 100$ nm and the unit of energy $E^* = \epsilon_1 = \pi^2\hbar^2/(2m^*a^2) = 1.0$ meV (i.e. the first lateral level of the quantum wire without SOC), the time unit $t^* = \hbar/E^* = 6.3 \times 10^{-13}$ s and the frequency unit $\Omega^* = 1/t^* = 1.6$ THz. With these units, the propagating longitudinal wavevector corresponding to the nth transverse mode is $k_x = (\omega - n^2)^{1/2}$. In the wide-band approximation the real part of the self-energy is negligible [22, 24–26], and we simply assume that $\Sigma_{11} = \Sigma_{22} = 0.1$ and $\Sigma_{12} = \Sigma_{21} = 0.05$. The choice of these typical parameters is based on the following consideration [22]. Usually the strength of electron–photon interaction depends on the photon intensity, polarization and the size of the quantum wire. Under the irradiation of a strong laser with an electric field of the order (10^5–10^6) V m^{-1}, the MEs are comparable to or several times larger than the level spacing in the quantum wire with the width of order (10–100) nm, and these quantities are physically realizable in recent experiments [18, 19].

We first consider the electronic structure of the system. It is commonly known that the electronic energy spectrum is degenerate for the two spin orientations in the absence of SOC. In the presence of SOC the energy spectrum (7) satisfies the condition $\varepsilon_{n,s}(k_x) = \varepsilon_{n,-s}(-k_x)$ in accordance with the time inversion symmetry. However, our interest is the interplay effect of the external laser field and the Rashba SOC on the electronic structure and transport of the system. Here we consider that the incident field is linearly polarized perpendicular to the current direction (the wire direction); i.e., the off-diagonal MEs dominate the electron–photon interaction. With the assumption of the off-diagonal MEs $V_{12} = V_{21} = 1.0$ (see equation (12)) and the incident laser frequency $\Omega = 0.5$, in figure 1 we illustrate the time-averaged DOS as a function of energy for the two different Rashba SOC strengths $k_{\mathrm{R}} = 1/(2\pi)$ and $k_{\mathrm{R}} = 1/\pi$, respectively. We can see that the main peak around $\omega \sim 1$ is always obvious in the presence of both Rashba SOC and laser field. This is because the electrons are populated at energy level $\varepsilon_{1\uparrow} \sim 1.01$ rather than $\varepsilon_{1\downarrow} \sim 1.25$ with single photon absorption. In the case of weak Rashba SOC strength as shown in figure 1(a), there are two additional photon resonance peaks at $\omega = 1.6$ and 4.6 for spin up (solid line), while for spin down (dashed line) there are three additional resonance peaks at $\omega = 4.58$, 0.75 and 0.65 with a pattern of oscillation in the range of $0.76 < \omega < 1$. Nevertheless, with the increase of the Rashba SOC strength shown in figure 1(b), for spin up the two photon resonance peaks are shifted from $\omega = 1$ and 4 to $\omega = 0.63$ and 3.4, respectively, while for spin down there only two resonance peaks occurring at $\omega = 0.63$ (superposed with that for spin up) and 3.5 without an oscillatory pattern. However, it seems that the other main peak around $\omega \sim 4$ makes sense in this strong Rashba SOC case. Because the single photon energy Ω is much smaller than the quantum wire sublevel spacing $\Delta\epsilon$, the resonance peaks here belong to the transitions between Rashba SOC-split subbands with the same lateral confinement quantum number [21].

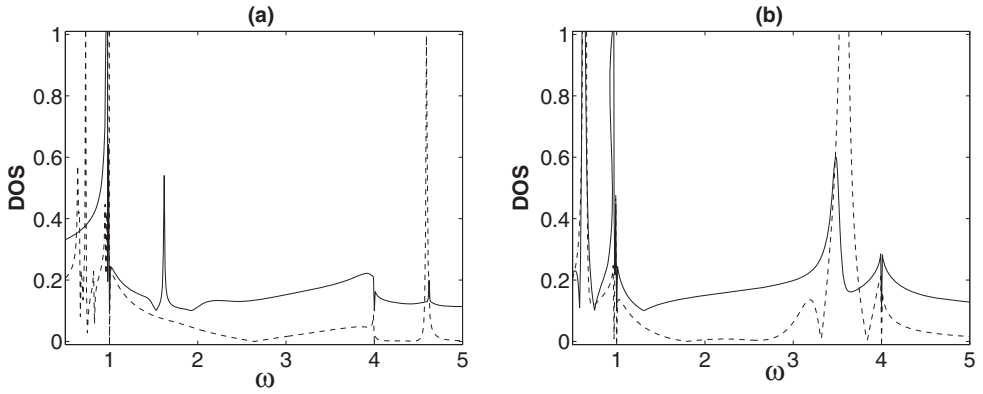

Figure 1. The time-averaged DOS (in arbitrary units) as a function of total energy ($\sim\omega$, in the unit of $\epsilon_1 = 1.0$ meV) with electron–photon interaction off-diagonal matrix elements $V_{1s2s'} = V_{2s1s'} = 1.0$ for the two different Rashba SOC strengths (a) $k_R = 6.74 \times 10^6$ m^{-1} and (b) $k_R = 1.35 \times 10^7$ m^{-1}, where the incident laser frequency is $\Omega = 0.8$ THz and the solid (dashed) line represents the spin up (down), shifted 0.1 upward for clarity.

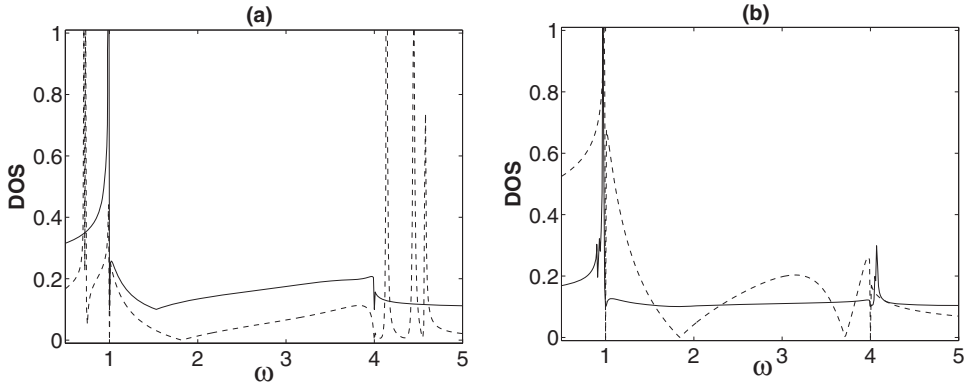

Figure 2. The time-averaged DOS (in arbitrary units) as a function of total energy with the same system parameters and line presentation as in figure 2, except that the incident laser energy is $\Omega = 4.8$ THz.

In order to determine the transitions between subbands with different confinement quantum numbers, in figure 2 we increase the incident frequency to $\Omega = 3$ but with the same two different Rashba SOC strengths as in figure 1. As shown in figure 2 the time-averaged DOS for spin up (solid lines) has no transition resonance peaks in both weak and strong Rashba SOC cases, while for spin down there are several sharp resonance transition peaks at $\omega = 0.75$, 4.1, 4.5 and 4.6 in the weak Rashba SOC case (see the dashed line in figure 2(a)) and an oscillatory pattern with no resonance peak (dashed line in figure 2(b)) in the strong Rashba SOC case. This result implies a rule of possible transition that the transition probabilities are much larger for this condition. We believe that some of the resonance peaks in figure 2(a) can be identified with the photon-induced transitions between subbands with different quantum numbers [21–23]. Because both spin-flip and spin-conserving transitions are modulated by the strengths of Rashba SOC and laser field, it seems that the strong strength of Rashba SOC in the higher laser frequency case is not favourable for the transitions between subbands with different quantum numbers.

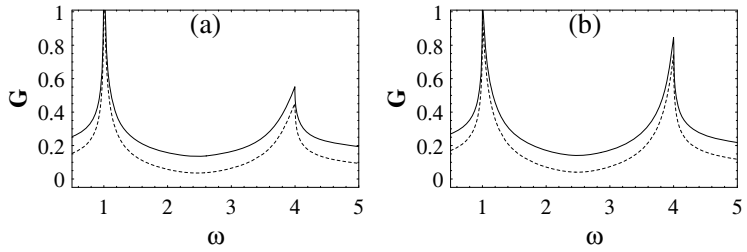

Figure 3. The plotted conductance G (in the unit of e^2/h) as a function of total energy ($\sim\omega$, in the unit of $\epsilon_1 = 1.0$ meV) without laser field for the two different Rashba SOC strengths (a) $k_R = 6.74 \times 10^6$ m^{-1} and (b) $k_R = 1.35 \times 10^7$ m^{-1}, where the solid (dashed) line represents the spin up (down), shifted 0.1 upward for clarity.

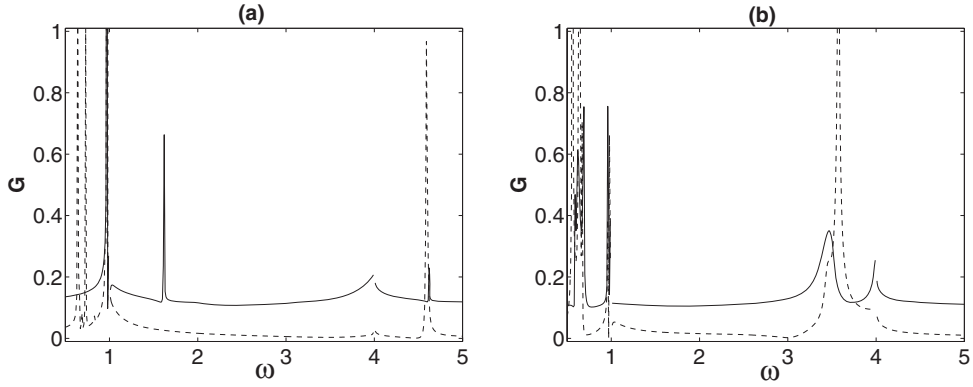

Figure 4. The time-averaged conductance G (in the unit of e^2/h) as a function of total energy with the same system parameters and line presentation as in figure 1.

Next we turn our attention to the conductance of the system. The conductance (in the unit of e^2/h) as a function of energy ($\sim\omega$, in the unit of ϵ_1) of the system without external laser field in the presence of weak and strong Rashba SOC is illustrated in figure 3. There are two major peaks in the conductance curves, as a consequence of the two subband level structure of the wire. In particular, the conductance difference for the two spin orientations in figure 3 is very small and consistent with the analytical prediction from the energy spectrum. One also notes that the conductance peaks are asymmetric near the two subband levels due to the spin–orbit interaction [26].

The time-averaged conductance of the system irradiated under a transversally polarized laser field in the presence of Rashba SOC is shown in figure 4 with $\Omega = 0.5$. Corresponding to the resonance states in figure 1(a), the time-averaged conductance in figure 4(a) shows some peaks with the height of $\sim e^2/h$. When the incident electron energy is about $\omega = 0.65$ and 0.75, we note that the conductance is nearly e^2/h for spin down while that for spin up is nearly zero; when the incident electron energy is increased to $\omega = 1.6$, there is a sharp conductance peak for spin up while that for spin down is about zero. Therefore, with a largest spin polarization in figure 1(a), a spin filter may be devised in the case of appropriate incident electron energy and Rashba SOC strength. Figure 4(b) shows the time-averaged conductance corresponding to figure 1(b) in the strong Rashba SOC case, from which one can see more photon resonance peaks (especially in lower energy range) than in the weak Rashba SOC case. Furthermore,

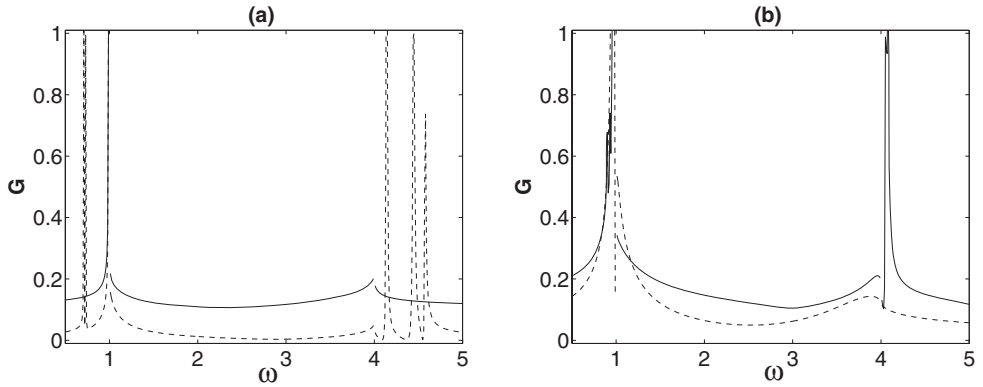

Figure 5. The time-averaged conductance G (in the unit of e^2/h) as a function of total energy with the same system parameters and line presentation as in figure 2.

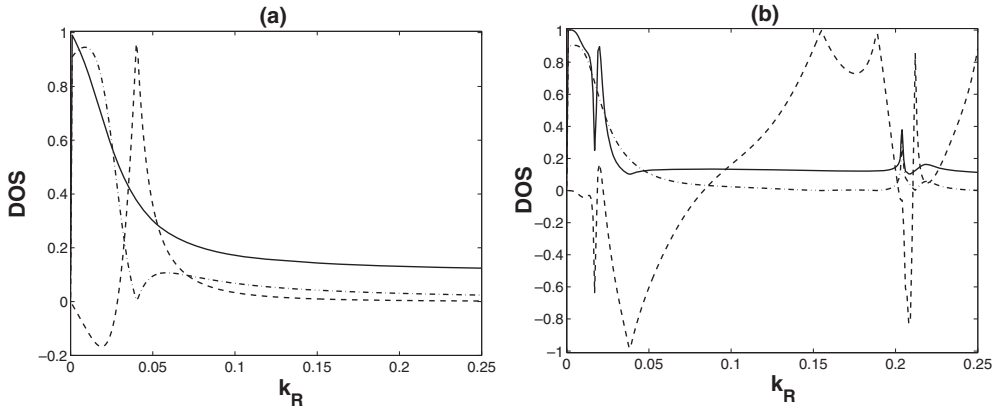

Figure 6. The time-averaged DOS and spin polarization rate as a function of k_R (proportional to the strength of Rashba SOC, in the unit of 4.2×10^7 m^{-1}) for a fixed incident electron energy $\omega = 2.5$ meV (a) without and (b) with a transversally polarized laser field ($\Omega = 0.8$ THz), with the solid line (shifted 0.1 upward for clarity) for spin-up and the dash–dotted line for spin-down DOS, respectively. The dashed line represents the spin polarization rate.

when the external laser frequency is increased to 3.0 the time-averaged conductance of the system with the two different Rashba SOC strengths is illustrated in figure 5. Due to the intersubband resonance states in figure 2(a), there are more sharp resonance transition peaks in a higher energy range (see figure 5(a)) for the spin-down electrons (see the explanation for figure 2(a)), while in the strong Rashba SOC case the conductance curves for both spin up and down show only the two main peaks (see figure 5(b)) as in figure 2(b). Maybe in this case the Rashba SOC is too strong to produce quantum transitions for the system.

Finally, the time-averaged DOS (solid line for spin up and dash–dotted line for spin down) and the spin polarization rate [20] (dashed line) with a fixed incident electron energy ($\omega = 2.5$) as a function of the characteristic wavevector k_R (proportional to the strength of Rashba SOC) without or with a transversally polarized external laser field ($\Omega = 0.5$) are demonstrated in figure 6(a) and (b), respectively. The electronic energy spectrum is degenerate for spin up and spin down when $k_R = 0$ in both cases as expected (see the solid and dash–dotted lines in

figure 6). In the case without a laser field as shown in figure 6(a), the spin polarization rate (dashed line) is about 17% when $k_R = 0.02$, and it can reach 95% when $k_R = 0.04$. Under the irradiation of the laser field, as shown in figure 6(b), the spin polarization rate increases to 60% and 100% around $k_R = 0.02$ and 0.04, respectively. Moreover, there are several additional peaks of spin polarization rate in the range of $0.05 < k_R < 0.25$ with laser field, while in the case without laser field as shown in figure 6(a) the spin polarization rate is smoothly low in this range of k_R. Therefore, it seems that the external laser field can enhance the spin polarization rate for a quantum wire system with an appropriate Rashba SOC strength, which can be adjusted through the controllable lateral electrodes [16].

4. Conclusion

In summary, using the method of EOM for the Keldysh NGF, we have investigated theoretically the electronic structure and transport properties of a two-sublevel quantum wire irradiated under a transversally polarized external laser field in the presence of the Rashba SOC. The time-averaged DOS and conductance for spin-up and spin-down electrons in the case of the off-diagonal electron–photon interaction dominating the process are calculated analytically, and are demonstrated numerically with two different Rashba SOC strengths and laser frequencies, respectively. It is found that the external laser field can enhance the spin polarization rate for the system with some particular Rashba SOC strengths. An all-electrical nonmagnetic spintronic device may be desirable under an appropriate choice of external control parameters. However, the experimental observation for this proposal and further theoretical investigation if the impurity, phonon or electron–electron interaction are taken into account are worth carrying out.

Acknowledgments

This work was supported by the National Natural Science Foundation of China (grant No 10574042), and by the Scientific Research Fund of Hunan Provincial Education Department (grant No 04A031).

References

[1] Zutic I, Fabian J and Sarma S D 2004 *Rev. Mod. Phys.* **76** 323
[2] Datta S and Das B 1990 *Appl. Phys. Lett.* **56** 665
[3] Mireles F and Kirczenow G 2004 *Phys. Rev.* B **64** 024426
Winkler R 2004 *Phys. Rev.* B **69** 045317
[4] Liu M-H, Chang C-R and Chen S-H 2005 *Phys. Rev.* B **71** 153305
[5] Governale M and Zülicke U 2002 *Phys. Rev.* B **66** 073311
[6] Onoda M and Nagaosa N 2005 *Phys. Rev. Lett.* **95** 106601
Onoda M and Nagaosa N 2005 *Phys. Rev.* B **72** 081301(R)
[7] Balents L and Egger R 2000 *Phys. Rev. Lett.* **85** 3464
Pramanik S, Bandyopadhyay S and Cahay M 2003 *Phys. Rev.* B **68** 075313
[8] Rodrigues V, Bettini J, Silva P C and Ugarte D 2003 *Phys. Rev. Lett.* **91** 096801
Wang X F, Vasilopoulos P and Peeters F M 2005 *Phys. Rev.* B **71** 125301
[9] Murakami S, Nagaosa N and Zhang S C 2003 *Science* **301** 1348
Murakami S, Nagaosa N and Zhang S C 2004 *Phys. Rev.* B **69** 235206
[10] Hirsch J E 1999 *Phys. Rev. Lett.* **83** 1834
Sinova J, Culcer D, Niu Q, Sinitsyn N A, Jungwirth T and MacDonald A H 2004 *Phys. Rev. Lett.* **92** 126603
Shen S-Q, Michael M, Xie X C and Fu C Z 2004 *Phys. Rev. Lett.* **92** 256603
[11] Bychkov Y A and Rashba E I 1984 *J. Phys. C: Solid State Phys.* **17** 6039

[12] Dresselhaus G 1955 *Phys. Rev.* B **100** 580
[13] Lommer G, Malcher F and Rössler U 1988 *Phys. Rev. Lett.* **60** 728
[14] Andradae Silva E A, Rocca G C L and Bassani F 1994 *Phys. Rev.* B **50** 8523
[15] Moroz A V and Barnes C H W 1999 *Phys. Rev.* B **60** 14272
[16] Nitta J, Akazaki T, Takayanagi H and Enoki T 2002 *Phys. Rev. Lett.* **78** 1335
Grundler D 2000 *Phys. Rev. Lett.* **84** 6074
Koga T, Nitta J, Akazaki T and Takayanagi H 2002 *Phys. Rev. Lett.* **89** 046801
[17] Sun Q-F and Xie X C 2005 *Phys. Rev.* B **71** 155321
Sun Q-F, Wang J and Guo H 2005 *Phys. Rev.* B **71** 165310
[18] Stevens M J, Smirl A L, Bhat R D R, Najmaie A, Sipe J E and van Driel H M 2003 *Phys. Rev. Lett.* **90** 136603
[19] Ganichev S D, Schneider P, Bel'kov V V, Ivchenko E L, Tarasenko S A, Wegscheider W, Weiss D, Schuh D, Murdin B N, Phillips P J, Pidgeon C R, Clarke D G, Merrich M, Murzyn P, Beregulin E V and Prettl W 2003 *Phys. Rev.* B **68** 081302(R)
[20] Najmaie A, Smirl A L and Sipe J E 2005 *Phys. Rev.* B **71** 075306
Sherman E Y, Najmaie A and Sipe J E 2005 *Appl. Phys. Lett.* **86** 122103
Cheng J L and Wu M W 2005 *Appl. Phys. Lett.* **86** 32107
[21] Fedorov A, Pershin Y V and Piermarocchi C 2005 *Phys. Rev.* B **72** 245327
Pershin Y V and Piermarocchi C 2005 *Appl. Phys. Lett.* **86** 212107
[22] Niu C and Lin D L 1997 *Phys. Rev.* B **56** R12752
Niu C and Lin D L 2000 *Phys. Rev.* B **62** 4578
[23] Zhou G, Yang M, Xiao X and Li Y 2003 *Phys. Rev.* B **68** 155309
[24] Meir Y and Wingreen N S 1992 *Phys. Rev. Lett.* **68** 2512
Jauho A P, Wingreen N S and Meir Y 1994 *Phys. Rev.* B **50** 5528
[25] Lee M and Bruder C 2005 *Phys. Rev.* B **72** 045353
Lee M and Choi M S 2005 *Phys. Rev.* B **71** 153306
[26] Yang M and Li S S 2004 *Phys. Rev.* B **70** 045318
[27] Chen G H and Raikh M E 1999 *Phys. Rev.* B **60** 4826